Electrical Power and Energy Systems 130 (2021) 106843

Contents lists available at ScienceDirect

International Journal of Electrical Power and Energy Systems

journal homepage: www.elsevier.com/locate/ijepes

Review

Probabilistic power flow for multiple wind farms based on RVM and holomorphic embedding method

Chenbo Su, Chongru Liu *, Siwen Jiang, Yu Wang

State Key Laboratory for Alternate Electrical Power System with Renewable Energy Sources, North China Electric Power University, Beijing, China

ARTICLE INFO

Keywords:
RVM
Correlation
PPF
Holomorphic Embedding

ABSTRACT

Wind power generation provides a new route for the sustainable development of energy. However, there is a correlation between wind speed in different regions, which will impact wind power and the stability of the power system. Therefore, it is necessary to estimate the steady-state characteristics of power systems and calculate probabilistic power flow (PPF) by considering this correlation. However, the traditional PPF calculation method based on the Newton–Raphson method may suffer from divergence or slow convergence with a high penetration of distributed energy resources. In this study, a new approach based on the relevance vector machine (RVM) was proposed to construct the multivariate copula in order to calculate the multivariate distribution of wind speed. By using the Rosenblatt transformation, the independent wind power variables could be obtained. After that, the cumulant method based on holomorphic embedding was proposed, which could acquire more accurate probability distribution results. The proposed novel method is evaluated on small, medium, and large power flow test cases and compared favorably with the popular PPF methods(such as NR method) on the same platform. Besides, the obtained results illustrated the advantages of the proposed method.

1. Introduction

Due to environmental deterioration and the exhaustion of fossil fuels, wind power has attracted significant attention worldwide as a clean and renewable energy source. This has led to a large quantity of installed capacity. The intermittent and random characteristics of wind power are mainly caused by the probabilistic property of wind speed, which can disrupt the stability of the power system and create new challenges due to drastically increasing uncertainties [1,2]. The purpose of probabilistic power flow (PPF) is to incorporate uncertainties into the power flow problem under various system conditions [3].

Existing analytical methods generally include the Monte Carlo method (MCM) [4,5], the point estimation method (PEM) [6,7], and the cumulant method [8,9]. MCM is widely used due to its simplification and accuracy. However, the time consumption of the MCM grows exponentially with an increase in the dimension of input variables. The point estimation method is efficient, but there is a decline in accuracy when the order of moments increases [6]. The cumulant method can accurately estimate the probability density function (PDF) with the series expansions [10]. However, the conventional cumulant method must first linearize power flow equations, which are generally based on the Newton–Raphson method [11]. In most cases, traditional PPF methods converge to the operable solution. However, these iterative methods may suffer from divergence or slow convergence with high penetration of distributed energy resources. When divergence under a numerical method occurs, two significant issues arise [12]:

(1) The numerical method fails to converge to a solution from the given start or.
(2) No solution exists, but the numerical method cannot detect its nonexistence.

In order to approach the above problem, a novel non-iterative method, known as the holomorphic embedding (HE) method, was proposed by Dr. Antonio Trias in 2012. A significant advantage of this method is that it is guaranteed to find a solution if it exists. The HE method will only find the operable solution and will unequivocally signal if no solution exists through oscillations in the rational approximation of the voltage power series [13]. Rao introduced one possible PV bus model compatible with the HEM and examined some features of different holomorphic embeddings [14]. In [15], the HE method was applied to DC power systems and nonlinear DC circuits. The system was devised by separating the series branch part from the shunt part of an admittance matrix, which generalized for the multi-bus problem. HE

* Corresponding author.

https://doi.org/10.1016/j.ijepes.2021.106843
Received 11 September 2020; Received in revised form 4 December 2020; Accepted 20 January 2021
Available online 23 March 2021

method was further extended to develop a multi-dimensional holomorphic embedding method in [16], which derived the analytical multivariate power series from approaching accurate power flow solutions. Moreover, a restarted HE method [17] was proposed to reduce the number of coefficients of the Padé approximant series and provided an efficient way to calculate the load-flow. In a word, the HE method has been applied to solve the power flow problem with absolute success. For the power grid with multivariate wind farms, this paper proposes a new analytical cumulant based on the HE method for accurate estimation of probability distributions for system variables.

In addition, the nonlinear correlation of wind speed between different regions is also of importance to estimate steady-state characteristics of power systems and calculate probabilistic power flow (PPF) [18]. Since the rank correlation index and tail correlation index of copula can better describe the nonlinearity, asymmetry, and upper and lower tail relationship between wind speed [5], the selection of a copula model is essential. However, it is difficult for the traditional copula to build a nonlinear correlation of multi-dimensional variables. Vine copula [19] represents a more flexible and simple method of extending bivariate conditional copula to multivariate dimensions. Nevertheless, the accuracy of multivariate joint distribution constructed by vine copula depends on the bivariate conditional probability density function (PDF) and marginal distribution [20]. Most studies in the literature used single-copula function from the elliptical copula family or the Archimedean copula family [21,22]. Typical representatives are the normal, Clayton, Frank, Gumbel, and Joe copulas [21]. However, the characteristics of asymmetry and tail correlation cannot always be described satisfactorily by using these copulas. A mixed copula [23] is a kind of copula function that consists of several different types of copula. It is prospectively able to reflect more characteristics of joint distribution since it includes more characteristics of copula functions. However, the general way to construct a mixed copula is parameter estimation, which restricts its accuracy.

In this paper, a new multivariate copula based on the relevance vector machine (RVM) is proposed, which is constructed by the Multiple-kernel function (Gaussian kernel and Polynomial kernel) in place of parameter estimation. Thus, it is of significant importance to model the multivariate copula of wind speed between wind farms and effectively improve accuracy. Besides, RVM is an extremely sparse Bayesian learning method, which can both effectively solve the problem of overfitting, as well as shorten the computing time. According to multivariate copula and Rosenblatt transformation, the wind power sequence P_w with independent distribution can be obtained, which will be used as the inputs of the cumulant method. Moreover, this paper also investigates a new analytical cumulant established by the HE method. Superior to existing PPF methods, the new approach is able to retain more accurate results of probability distributions.

The rest of this paper is organized as follows. In Section 2, the related RVM methods and the way to construct the multivariate copula of wind speed are introduced in detail. In Section 3, the cumulant method based on holomorphic embeddings is explained. In Section 4, an application of the proposed methods for the calculation of PPF with multi-dimensional wind farms is presented. In Section 5, the work of this paper is summarized, and the conclusions are given.

2. Model of multivariate distributions for wind farms

Sklar has demonstrated the relationship between the joint distribution function *F*, the multivariate copula *C,* and the marginal cumulative distribution function (CDF) *Fi* [24]. This theory provides a convenient way to model multivariate distributions for the multiple wind farm case.

2.1. The basis of R-Vine copula

As a derivation of the copula function, regular vine, as given by Bedford [25], is a graphical model used to determine the structure of the R-vine copula, which provides an efficient way to establish multivariate distribution based on bivariate copula and marginal distribution. In the context of R-vine copulas, each edge corresponds to a bivariate copula. And according to the definition [25], R-vine consists of tree T_i with nodes N_i and edges E_i, for $i = 1,\ldots,d\text{-}1$, and several conditions should be satisfied:

1) The node N_i and the edge E_i belong to tree T_i.
2) The node N_i of tree T_i is equal to the edge $E_{i\text{-}1}$ in $T_{i\text{-}1}$, which means: $N_i = E_{i\text{-}1}$, for $i = 1,\ldots,d\text{-}1$.
3) If one edge in tree T_i is connected with another edge in tree T_{i+1}, these two edges share a common node in tree T_i.

According to the definition of R-vine, assuming a *d*-dimensional random vector $\boldsymbol{X} = [X_1, X_2, \ldots, X_d]$, and setting f_k to be the marginal density of the variable X_k, the joint PDF $f(x_1, x_2, \ldots, x_d)$ can be described as:

$$f(x_1, x_2, \ldots, x_d) = \prod_{l=1}^{d} f_l(x_l) \times \prod_{i=1}^{d-1} \prod_{e \in E_i} \widehat{c}_{j(e),k(e)|D(e)} \times \left(F\left(x_{j(e)}\middle|x_{D(e)}\right), F\left(x_{k(e)}\middle|x_{D(e)}\right)\right) \tag{1}$$

where an edge $e = j(e),k(e)|D(e)$ belongs to E_i, $j(e)$, $k(e)$ are two conditional nodes of edge e, and $D(e)$ is the condition set. $\widehat{c}_{j(e),k(e)|D(e)}$ is a PDF of conditional bivariate copula, which is derived from (1). Also, the conditional CDF $F(x_{j(e)}|x_{D(e)})$ in (1) can be calculated by:

$$F\left(x_{j(e)}\middle|x_{D(e)}\right) = \frac{\partial C\left(F\left(x_{j(e)}\right), F\left(x_{D(e)}\right)\right)}{\partial F\left(x_{D(e)}\right)} \tag{2}$$

Generally, most studies construct the bivariate copula in (2) through single-copula and mix-copula [26,27]. In order to obtain their relevant parameters, the usual way is maximum likelihood estimation (MLE). However, it lacks accuracy for modeling the copula of wind speed via parameter estimation. Also, with the rise of variable dimension, the number of parameters that need to be estimated increases exponentially; thus, it will cause the complication of calculation and consume too much time. Due to these potential problems, the implementation of RVM on modeling multivariate copula is proposed in this paper.

2.2. A new multivariate copula based on RVM

Since RVM is a kernel learning method derived from Bayesian theory, it constructs a basis function in place of parameter estimation. RVM also provides the following advantages:

(1) RVM is an extremely sparse Bayesian learning method, which can effectively solve the problem of overfitting and shorten computing time.
(2) It is a machine learning method based on kernel function, which can effectively avoid dimension disaster when building a high-dimensional nonlinear model.

2.2.1. The fundamental of RVM

According to Tipping's study [28], suppose a training data set $\{\boldsymbol{x}_i, t_i\}_{i=1}^{N}$, $\boldsymbol{x}_i$ and t_i are the input vector and the corresponding target, respectively. Thus, the definition of target t_i is shown as follow:

$$t_i = y(\boldsymbol{x}_i; \boldsymbol{\omega}) = \sum_{k=1}^{N} \omega_{ik} K(\boldsymbol{x}_i, \boldsymbol{x}_k) + \omega_{i0} + \varepsilon_i \tag{3}$$

where $K(\boldsymbol{x_i}, \boldsymbol{x_k})$ is the kernel function, $\boldsymbol{\omega} = (\omega_1, \omega_2, \ldots, \omega_n)^T$ represents the weight vector, and ε_i is the noise. And the likelihood of $\boldsymbol{\omega}$ is defined as follows:

$$p(\boldsymbol{t}|\boldsymbol{\omega},\sigma^2) = (2\pi\sigma^2)^{-\frac{N}{2}}exp\left\{-\frac{1}{2\sigma^2}\|\boldsymbol{t}-\boldsymbol{\omega\phi}\|\right\} \tag{4}$$

where $\boldsymbol{\phi} = (\phi(\boldsymbol{x_1}), \phi(\boldsymbol{x_2}),\ldots, \phi(\boldsymbol{x_N}))$, and $\phi(\boldsymbol{x_i}) = [1, K(\boldsymbol{x_i}, \boldsymbol{x_1}), K(\boldsymbol{x_i}, \boldsymbol{x_2}), \ldots, K(\boldsymbol{x_i}, \boldsymbol{x_N})]^{\mathrm{T}}$ represents kernel function. In this paper, the input vector $\boldsymbol{x_i}$ is sampled from different wind speed sequences $V = (v_1,v_2,\ldots,v_N)$ of wind farms. The maximum-likelihood estimations of $\boldsymbol{\omega}$ and σ^2 may result in an over-fitting phenomenon. So, the zero-mean Gaussian weight-prior probability distribution is employed to constrain these two parameters.

$$p(\boldsymbol{\omega}|\boldsymbol{\alpha}) = \prod_{i=0}^{N} N(\omega_i|0,\alpha_i^{-1}) \tag{5}$$

2.2.2. The structure of proposed multivariate copula

According to Bayesian theory, the posterior probability distribution is equal to the weight-prior multiplied maximum likelihood estimation. Thus, the posterior probability distribution $p(\boldsymbol{\omega}|\boldsymbol{t}, \sigma^2,\boldsymbol{\alpha})$ takes the form:

$$\begin{gathered} p(\boldsymbol{\omega}|\boldsymbol{t},\boldsymbol{x_n},\sigma^2,\boldsymbol{\alpha}) = \frac{p(\boldsymbol{t}|\boldsymbol{\omega},\boldsymbol{x_n},\sigma^2)p(\boldsymbol{\omega}|\boldsymbol{\alpha})}{p(\boldsymbol{t}|\boldsymbol{x_n},\sigma^2,\boldsymbol{\alpha})} = \\ (2\pi)^{-\frac{N+1}{2}}|\Sigma|^{-\frac{1}{N}}exp\left\{-\frac{(\boldsymbol{\omega}-\boldsymbol{\mu})^T\Sigma^{-1}(\boldsymbol{\omega}-\boldsymbol{\mu})}{2}\right\} \\ \boldsymbol{\mu} = \sigma^2\ \Sigma\phi(\boldsymbol{x_n})^T\boldsymbol{t} \\ \Sigma = \left(\boldsymbol{A}+\sigma^2\ \ \phi^T(\boldsymbol{x_n})\phi(\boldsymbol{x_n})\right)^{-1} \end{gathered} \tag{6}$$

where $\mathbf{A} = diag(\alpha_i)$, σ is the covariance of $\boldsymbol{x_n}$, and $\boldsymbol{t}(t_1,t_2,\ldots,t_n)^T$ sampled from C_n is called the multivariate empirical copula which is derived from the bivariate empirical copula C_b and R-Vine structure. The expression of C_b is given as follow :

$$C_b(F_1(\boldsymbol{v}_1),F_2(\boldsymbol{v}_2)) = \frac{1}{N}\sum_{j=1}^{N} I_{[F_1(v_{1j})\leqslant F_1(v_{1i})]}I_{[F_2(v_{2j})\leqslant F_2(v_{2i})]} \tag{7}$$

where $I[\cdot]$ is an indicator function. If $F_1(v_{1j}) < F_1(v_{2i})$, $I = 1$; otherwise, $I = 0$. Besides, The matrix $V= (\boldsymbol{v}_1,\boldsymbol{v}_2,..,\boldsymbol{v}_N)^{\mathrm{T}}$ represents different wind speed sequences derived from historical data. The marginal cumulative distribution of $\boldsymbol{v}_1$ and $\boldsymbol{v}_2$ are $F_1(\boldsymbol{v}_1)$ and $F_2(\boldsymbol{v}_2)$, respectively. By substituting (7) into (1) and, we obtain.

$$\begin{aligned} C_n(F_1(\boldsymbol{v}_1),\cdots,F_N(\mathbf{v}_N)) = \prod_{k=1}^{N}\mathrm{f_k}(\mathbf{v}_k)\cdot\prod_{j=1}^{N-1}\prod_{i=1}^{N-j}\mathrm{C}_{bi,i+j|i+1,\cdots,i+j-1} \\ \cdot\left(F_{i|i+1,\cdots,i+j-1}\left(\boldsymbol{v}_i|\boldsymbol{v}_{i+1},\cdots,\boldsymbol{v}_{i+j-1}\right),\right. \\ \left.F_{i+j|i+1,\cdots,i+j-1}\left(\boldsymbol{v}_{i+j}|\boldsymbol{v}_{i+1},\cdots,\boldsymbol{v}_{i+j-1}\right)\right) \end{aligned} \tag{8}$$

where the conditional CDF $F_{i|j}(v_i|v_j)$ can be calculated by (2).

Since the regression performance of RVM is dependent on the kernel function, in this paper, the Multiple-kernel function (Gaussian kernel and Polynomial kernel) apply to construct the multivariate copula.

Gaussian kernel function has an extensive implementation for its excellent performance in dealing with nonlinear data [29], and the function can be expressed as follows:

$$K_G(\boldsymbol{x}_i,\boldsymbol{x}_N) = exp\left(-\frac{\|\boldsymbol{x}_i-\boldsymbol{x}_N\|}{2\theta^2}\right) \tag{9}$$

where the θ is the kernel width. The polynomial kernel function is proven to be an effective supplement to the Gaussian kernel function [30]. This function is described as:

$$K_p(\boldsymbol{x}_i,\boldsymbol{x}_N) = \left[\boldsymbol{x}_N^T\cdot\boldsymbol{x}_i+1\right]^n \tag{10}$$

where n is the degree. The definition of multiple-kernel is:

$$K(\boldsymbol{x}_i,\boldsymbol{x}_N) = \varphi K_G(\boldsymbol{x}_i,\boldsymbol{x}_N) + \gamma K_G(\boldsymbol{x}_i,\boldsymbol{x}_N) \tag{11}$$

where $\varphi+\gamma = 1$. In this work, the coefficient φ and γ of multiple-kernel are derived from the Weibull distribution, which is closer to the actual distribution of wind speed [31]. The expression is shown as follow:

$$f(\boldsymbol{x}_i,\lambda,\zeta) = \frac{\zeta}{\lambda^k}\boldsymbol{x}_i^{\zeta-1}e^{-(\boldsymbol{x}_i/\lambda)^\zeta} \tag{12}$$

where λ and ζ are the scale parameter and the shape parameter, respectively, thus, the specific procedures of coefficient optimization are given as follow:

*Step*1: Generate the scale parameter λ and the shape parameter ζ from the actual wind speed sequence.

*Step*2: Get the coefficient φ and γ from minimizing the Kullback-Leibler (K-L) divergence [32] of multiple-kernel and Weibull distribution. And the expression of K-L divergence is given as follow:

$$D_{KL}(f||\mathrm{K}) = \sum_{i=1}^{N} f(\boldsymbol{x}_i)\cdot(logf(\boldsymbol{x}_i) - logK(\boldsymbol{x}_i,\overline{\boldsymbol{\mu}})) \tag{13}$$

where $f(\boldsymbol{x_i}) = f(\boldsymbol{x_i}, \lambda, \zeta)$, Î¼ $= 1/\mathrm{N}\sum_{i=1}^{N}\mathrm{x_i}$. Furthermore, the α_i and β in (6) can be obtained by iteration.

$$\begin{gathered} \alpha_i^{new} = \frac{1-\alpha_i\Sigma_{ii}}{\mu_i^2} \\ \sigma_{new}^2 = \frac{||C_n(F_1(\boldsymbol{v}_1),F_2(\boldsymbol{v}_2)\cdots,F_N(\mathbf{v}_N)) - \boldsymbol{\phi}\ \boldsymbol{\mu}||^2}{N-\sum_i(1-\alpha_i\Sigma_{ii})} \end{gathered} \tag{14}$$

where μ_i is the i_{th} component of the posterior mean $\boldsymbol{\mu}$, Σii is the ith diagonal component of the posterior covariance $\boldsymbol{\Sigma}$ given by (4). By substituting α_i and σ^2 obtained by iteration into Eq. (6), we can get the correction equation of weight coefficient $\boldsymbol{\omega}$. Therefore, multivariate copula based on RVM can be expressed as :

$$C_i^{RVM}(\boldsymbol{\eta}_i) = \sum_{k=1}^{N}\omega_{ik}K(\boldsymbol{\eta}_i,\boldsymbol{\eta}_k) + \omega_{i0} \tag{15}$$

where, $\boldsymbol{\eta}_i= (F_{1i}(\boldsymbol{v}_1), F_{2i}(\boldsymbol{v}_2),\ldots, F_{Ni}(\boldsymbol{v}_N))^{\mathrm{T}}$ represents the ith vector of marginal distribution of wind speed sequences $V= (\boldsymbol{v}_1,\boldsymbol{v}_2,..,\boldsymbol{v}_N)^{\mathrm{T}}$.

To conclude, there are two critical advantages of RVM. On the one hand, it utilizes the Multiple-kernel function in place of parameters estimation, which is more significant for an accurate model of the multivariate distribution of wind farms. On the other hand, a separate hyperparameter α_i for each of the weight parameters ωi is introduced instead of a single shared hyperparameter. During the calculation, a considerable proportion of $\boldsymbol{\alpha}$ will extend to infinity, and the posterior distributions of $\boldsymbol{\omega}$ will be concentrated at zero. Therefore, $\boldsymbol{\alpha}$ becomes a sparse model, which will significantly reduce the computation time.

2.2.3. To obtain the independent power sequences of wind farms via proposed method

However, the multivariate distribution with correlation cannot be used to compute the power of wind farms directly. Thus, Rosenblatt transformation [33] is utilized to convert input wind speed sequences with correlation into independent variables. Then, the power of a wind generator can be calculated by

$$f(\boldsymbol{x}_i,\lambda,\zeta) = \frac{\zeta}{\lambda^k}\boldsymbol{x}_i^{\zeta-1}e^{-(\boldsymbol{x}_i/\lambda)^\zeta} \tag{16}$$

where *vwi*, *vwo*, and *vr* are the cut-in, cut-out, and nominal wind speed, respectively. Thus, the independent power of wind farms P_w derived from Rosenblatt transformation can be used for the calculation of PPF. Above all, the proposed method can be introduced to obtain realistic results.

3. Cumulants based on holomorphic embedding

Generally, the power flow equation at PQ bus i can be expressed in the rectangular coordinates, namely:

$$\sum_{j=1}^{N} Y_{ij} V_k = \frac{S_i^*}{V_i^*} \tag{17}$$

where S_i represents the power injection at bus i, supposing V_j is the voltage at bus j, and $S_i = P \pm jQ$ is a complex number. Besides, the power flow equation of the PV bus i is given by:

$$\begin{cases} |V_i| = V_i^{sp} \\ P_i = Re\left(V_i \sum_{j=1}^{N} Y_{ij}^* V_k^*\right) \end{cases} \tag{18}$$

3.1. Holomorphic embedding PQ model

The HE method can be applied to solve the power flow problem with the complex-valued parameter s [14].

$$\begin{aligned} \sum_{j=1}^{N} Y_{ij,trans} V_j(s) &= \frac{sS_i^*}{V_i^*(s^*)} - sY_{i,shunt} V_i(s) \\ V_i(s) &= a_{i0} + a_{i1}s + \cdots + a_{in}s^n \\ V_i^*(s^*) &= a_{i0}^* + a_{i1}^* s + \cdots + a_{in}^* s^n \end{aligned} \tag{19}$$

where *Yik,trans* and *Yi,shunt* are the series-branch part and shunt part, respectively, of the admittance matrix Y, and Qi is the reactive power. a_{in}^* is the conjugate of the power series coefficient a_{in}. In order to find the series of coefficients that satisfy (19), let the inverse of voltage function $V_i(s)$ be expressed by $W_i(s)$. We then have:

$$\begin{aligned} W_i(s) &= \frac{1}{V_i(s)} \\ W_i(s) &= b_{i0} + b_{i1}s + \cdots + b_{in}s^n \end{aligned} \tag{20}$$

The product of the two power series $V_i(s)$ and $W_i(s)$ is the convolution of their coefficients. Therefore, the relationship of coefficients a_{in} and b_{in} is given by [14]:

$$\begin{aligned} a_{i0} &= \frac{1}{b_{i0}} \\ a_{i1}b_{i0} + b_{i1}a_{i0} &= 0 \\ a_{i2}b_{i0} + b_{i1}a_{i1} + a_{i0}b_{i2} &= 0 \\ &\vdots \\ b_{in} &= -\frac{\sum_{k=0}^{n-1} b_{ik}a_{i(n-k)}}{a_{i0}} \end{aligned} \tag{21}$$

By substituting (21) into (19) and (20), we obtain:

$$\sum_{j=1}^{N} Y_{ij,trans} a_{jn} = S_i^* b_{i(n-1)}^* - Y_{i,shunt} a_{i(n-1)} \tag{22}$$

Therefore, the coefficients a_{in} and b_{in} can be obtained by the recurrence relation defined by Eqs. (21) and (22). Then the voltage series for load/PQ buses can be calculated.

3.2. Holomorphic embedding PV model

For the generator bus, both the voltage magnitude and real power are known quantities, and the reactive power and voltage angle are unknown. Q_i can be written as a power series expansion in the form of a complex number as below[15]:

$$\begin{aligned} \sum_{j=1}^{N} Y_{ij,trans} V_j(s) &= \frac{sP_i - jQ_i(s)}{V_i^*(s^*)} - sY_{i,shunt} V_i(s) \\ Q_i(s) &= q_{i0} + q_{i1}s + \cdots + q_{in}s^n \end{aligned} \tag{23}$$

To calculate the coefficients of the voltage and reactive power series for a generator bus model, Eqs. (21) and (22) are taken into (23).

$$\begin{aligned} \sum_{j=1}^{N} Y_{ij,trans} a_{jn} + jq_{in} &= P_i b_{i(n-1)}^* - j\left(\sum_{k=1}^{n-1} q_{ik} b_{i(n-k)}^*\right) \\ &\quad - Y_{i,shunt} a_{i(n-1)} \end{aligned} \tag{24}$$

Besides, the voltage-magnitude constraint in the HE method can be expressed as [15]:

$$V_i(s) \cdot V_i^*(s^*) = 1 + s\left(|V_i^{sp}|^2 - 1\right) \tag{25}$$

where V_i^{sp} is the specified voltage magnitude at the slack bus. Therefore, by substituting (18) and $a_{i0} = 1.0$ into (25), we can calculate the a_{in}, and the result is shown as follows:

$$a_{in,re} = \delta_{n0} + \delta_{n1} \frac{V_i^{sp2} - 1}{2} - \frac{1}{2}\left(\sum_{k=1}^{n-1} a_{ik} a_{i(n-k)}^*\right) \tag{26}$$

where $a_{in,re}$ represents the real part of the coefficients of the voltage power series. Above all, $Q_i(s)$ and $V_i(s)$ can be calculated by Eqs. (21), (24), and (26).

Moreover, the Padé approximant can provide better approximations within or beyond the power series radius of convergence [13]. Therefore, it can be utilized to compose numerical solutions for power flow. Note that the rational approximants can always be converted into an algebraic fraction in which the numerator and the denominator are both polynomials. Thus, the Padé approximant can be expressed as:

$$\begin{aligned} [L/M]_j(s) &= \frac{m_{j0} + m_{j1}s + \cdots + m_{jl}s^l}{n_{j0} + n_{j1}s + \cdots + n_{jm}s^m} \\ &= a_{j0} + a_{j1}s + \cdots + a_{jn}s^n \end{aligned} \tag{27}$$

where the integers L and M in $[L/M]_k(s)$ are the degrees of the polynomial in the numerator and the denominator, respectively. Generally, the value of L is equal to M. The coefficients m_{jn} and n_{jn} can be calculated by (27).

3.3. Cumulants based on HE method

The objective of using cumulants is to calculate the PPF of the power system. Suppose random variable X is subjected to PDF $f(x)$ or cumulative distribution function (CDF) $F(x)$. The characteristic function of X can be expressed as:

$$\psi(t) = E\left(e^{itX}\right) = \int_0^{+\infty} e^{itX} f(x) dx \tag{28}$$

where i is the imaginary unit, and t is a real number. The cumulants are derived from the expansion of $\psi(t)$. Besides, the coefficients α_v and β_v represent the vth order moment and the vth order central moment of X, which has the mean value μ.

$$\begin{aligned} \alpha_v &= E(X^v) = \int_0^{+\infty} x^v f(x) dx = \int_0^{+\infty} x^v dF(x) \\ \beta_v &= E[(X-\mu)^v] = \int_0^{+\infty} (x-\mu)^v dF(x) \end{aligned} \tag{29}$$

Therefore, according to [10], the vth cumulants κ_v have a relationship with α_v.

$$\begin{aligned}\kappa_1 &= \alpha_1 = \mu \\ \kappa_v &= \alpha_v - \sum_{i=1}^{v-1}\binom{v-1}{i-1}\kappa_i\alpha_{v-i}\end{aligned} \tag{30}$$

Since conventional cumulants are based on the NR method, we need to make some improvements in order to apply it to holomorphic embedding. Assuming that $\overline{P}$ and $\overline{Q}$ are the mean value of injected active power and reactive power, respectively, then the power flow can be expressed as follows:

$$\begin{aligned}\sum_{j=1}^{N} Y_{ij,trans}\overline{V}_j(s) &= \frac{s\overline{S}_i^*}{\overline{V}_i^*(s^*)} - sY_{i,shunt}\overline{V}_i(s) \\ \sum_{j=1}^{N} Y_{ij,trans}\overline{V}_j(s) &= \frac{s\overline{P}_i - j\overline{Q}_i(s)}{\overline{V}_i^*(s^*)} - sY_{i,shunt}\overline{V}_i(s)\end{aligned} \tag{31}$$

where the $\overline{V}_j$, $\overline{Q}_j$, and $1/\overline{V}_j^*$ can be obtained by:

$$\begin{aligned}\overline{V}_i(s) &= \overline{a}_{i0} + \overline{a}_{i1}s + \cdots + \overline{a}_{in}s^n \\ \overline{W}_i^*(s) &= 1\Big/\overline{V}_i^*(s) = \overline{b}_{i0}^* + \overline{b}_{i1}^*s + \cdots + \overline{b}_{in}^*s^n \overline{Q}_i(s) = \overline{q}_{i0} + \overline{q}_{i1}s + \cdots + \overline{q}_{in}s^n\end{aligned} \tag{32}$$

In order to find the appropriate germ, assume that the voltage magnitude of all generator buses is 1.0 at $s = 0$. Hence, the solution of (31) at $s = 0$ corresponds to a network with no load and no shunt element. This situation is selected as the germ of voltage, and the linear system of equations at $s = 0$ is given:

$$\begin{cases}\sum_{j=0}^{N} Y_{ij,trans}\overline{a}_{j0} = 0 \\ \sum_{j=0}^{N} Y_{ij,trans}\overline{a}_{j0} = \dfrac{-j\overline{q}_{i0}}{\overline{a}_{i0}^*}\end{cases} \tag{33}$$

If the Padé approximants converge at $s = 1$, the result is guaranteed to have the final solution. However, if there is no solution for the power flow, the value of the approximant oscillates. When $s = 1$, the results in (32) become:

$$\begin{aligned}A_i(1) &= \overline{V}_i(1) = \overline{a}_{i0} + \overline{a}_{i1} + \cdots + \overline{a}_{in} \\ B_i(1) = \overline{W}_i^*(1) &= \overline{b}_{i0}^* + \overline{b}_{i1}^* + \cdots + \overline{b}_{in}^* D_i(1) = \overline{Q}_i(s) = \overline{q}_{i0} + \overline{q}_{i1} + \cdots + \overline{q}_{in}\end{aligned} \tag{34}$$

By substituting (34) into (31), we have:

$$\sum_{j=1}^{N} Y_{ij}A_j(1) = \overline{S}_i^* \cdot B_i(1) \sum_{j=1}^{N} Y_{ij}A_j(1) = \left(\overline{P}_i - jD_i(1)\right)\cdot B_i(1) \tag{35}$$

In summary, the specific procedures of coefficient calculation are given as follow:

*Step*1: Generate the germ via (33).

*Step*2: Calculate $\overline{b}_{\text{in-1}}^*$ from $\overline{b}_{\text{ij}}^*$ ($j <$ n-1) and $\overline{a}_{\text{ij}}$ ($j <$ n-1) using (21)

*Step*3: For *P-Q* bus, calculate $\overline{a}_{\text{in}}$ from $\overline{b}_{\text{in-1}}^*$ and $\overline{a}_{\text{in-1}}$ via (22); For the generator bus, firstly, calculate the $\overline{a}_{\text{in,re}}$ from (26). Then, using $\overline{b}_{\text{in-1}}^*$, $\overline{a}_{\text{in-1}}$ and $\overline{a}_{\text{in,re}}$ to acquire $\overline{a}_{\text{in,im}}$ and $\overline{q}_{\text{in}}$ from (24).

*Step*4: Recursively apply steps 2 through 4

*Step*5: Substituting power series into Padé approximants until the accuracy requirements are met. Therefore, the solution of $A_i(1)$, $B_i(1)$, and $D_i(1)$ in (35) can be obtained.

Assuming that W and Z are the vectors of injected active power and reactive power at the bus and in the branch, respectively, the mean value of W is $\overline{W}$ and the mean value of Z is $\overline{Z}$. Additionally, let X be the bus voltage vector consisting of the real part and the imaginary part. According to Eq. (35), the relationship between $\overline{W}$, $\overline{Z}$, and $\overline{X}$ can be expressed as follows:

$$\begin{aligned}\overline{X} &= S_0\overline{W} \\ \overline{Z} &= G_0S_0\overline{W}\end{aligned} \tag{36}$$

Therefore, the vth cumulants of $\overline{Z}$ and $\overline{X}$ can be obtained from the vth cumulants of $\overline{W}$.

$$\begin{cases}\kappa_1^{\overline{X}} = S_0\kappa_1^{\overline{W}} = \mu_{\overline{X}} \\ \kappa_2^{\overline{X}} = S_0^2\kappa_2^{\overline{W}} \\ \vdots \\ \kappa_v^{\overline{X}} = S_0^v\kappa_v^{\overline{W}}\end{cases} \quad \begin{cases}\kappa_1^{\overline{Z}} = G_0S_0\kappa_1^{\overline{W}} + Z_{l0} = \mu_{\overline{Z}} \\ \kappa_2^{\overline{Z}} = G_0^2S_0^2\kappa_2^{\overline{W}} \\ \vdots \\ \kappa_v^{\overline{Z}} = G_0^vS_0^v\kappa_v^{\overline{W}}\end{cases} \tag{37}$$

where $Z_{l0} = Z_0 - G_0S_0W_0$. Thus, the PDF of the bus voltage and power in the branch can be calculated by power series expansion. Compared with Gram–Charlier expansion and Edgeworth expansion, Cornish–Fisher expansion has higher accuracy in dealing with the non-normal distribution of random variables [36]. Therefore, in this paper, the Cornish–Fisher series is applied to calculate the PPF of the power system. The first five orders of Cornish–Fisher expansion are shown as follows:

$$\begin{aligned}Y(q) = \tau(q) + \frac{\tau(q)-1}{6}\kappa_3 + \frac{\tau^3(q)-3\tau(q)}{24}\kappa_4 - \\ \frac{\tau^3(q)-5\tau(q)}{36}\kappa_3^2 + \frac{\tau^4(q)-6\tau^2(q)+3}{120}\kappa_5 + \cdots\end{aligned} \tag{38}$$

where $Y(q)$ is the quantile of the output, and $\tau(q)$ is the quantile of the standard normal distribution, $\tau(q) = \Phi^{-1}(q)$.

4. Numerical test

The proposed method was tested on different systems, which contain some practical grid in China, and the number of buses ranges from 14 to 3661. Therefore, these cases are enough to give a clear insight into the nature of the problem. Additionally, in this paper, wind speed data and its corresponding actual power output data from geographically close wind farms in China from 2016 to 2018 are used. Load fluctuation was

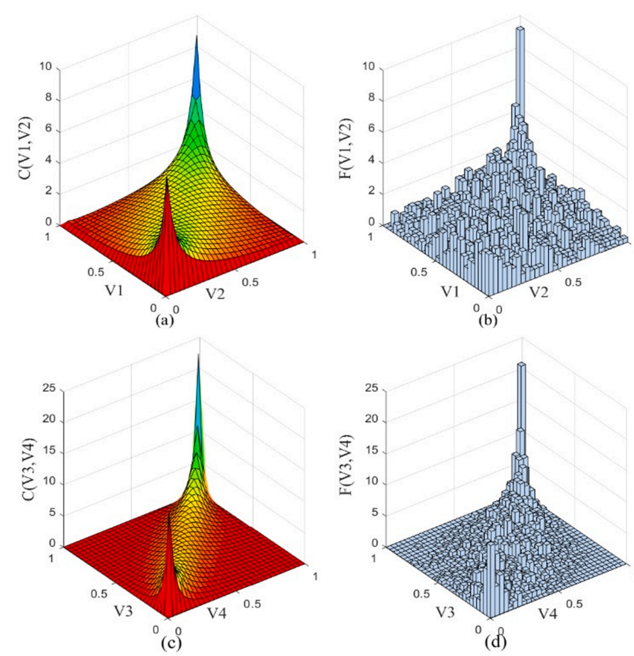

Fig. 1. Joint PDF of two groups of wind speeds.

Table 1
Comparison between different methods.

Method	Sample	d	K
C_{RVM} $(\nu_1, \nu_2, \nu_3, \nu_4)$	2555	1.9841	0.179
	8760	1.9624	0.178
	52,560	1.9536	0.178
C_{LSQ} $(\nu_1, \nu_2, \nu_3, \nu_4)$	2555	2.2143	0.195
	8760	2.1972	0.192
	52,560	2.2064	0.193
C_{EM} $(\nu_1, \nu_2, \nu_3, \nu_4)$	2555	2.1267	0.189
	8760	2.0742	0.185
	52,560	2.0053	0.183

assumed to be the normal distribution as well. Besides, all results were obtained using MATLAB.

Based on the actual data of four wind farms, the marginal distribution of each wind speed sequence could be obtained by the kernel estimation method. These marginal distributions will be used as the input variables of the proposed RVM method to construct the multivariate copula. And two groups of bivariate PDF generated by multivariate copula are applied to compare with the frequency histogram derived from the historical data, as illustrated in Fig. 1. From the plots, it is evident that the bivariate PDF is close to the frequency histogram.

In order to further study the performance of the proposed method, it was compared with the mix-copula, which can be expressed as (39), and its parameters ω and θ estimated by the expectation–maximization algorithm (EM) and least square method (LSQ), respectively.

$$C_m = \omega_1 C_T(F_1(x_1), F_2(x_2); \theta_1) + \omega_2 C_G(F_1(x_1), F_2(x_2); \theta_2) + \omega_3 C_c(F_1(x_1), F_2(x_2); \theta_3) \quad (39)$$

where $C_T(x)$, $C_G(x)$, and $C_C(x)$ represent T-Copula, Gumbel copula, and Clayton copula, respectively.

These two mix-copula based on parameter estimation was extended to multi-dimension via R-Vine structure. After that, The Kolmogorov–Smirnov (KS) test [40] and the Euclidean distance [41] were used for comparison. The results are presented in Table 1 and demonstrate that if the calculated distribution is close to the empirical distribution, the value of K and d will be small. According to the results, it can be concluded that no matter what the sampling value is, the multivariate copula based on RVM is much similar to the empirical copula employed in different research. Moreover, the size of the sampling space has little effect on the accuracy of the proposed method.

In Table 1, C_{RVM}, C_{LSQ}, and C_{EM} represent the multivariate copula based on RVM, LSQ, and EM, respectively.

The P-P diagrams in Fig. 2(a)–(c) are used to compare different multivariate copula by changing the sample number. As we can see, the P-P diagrams of three different estimation methods (including RVM, EM, and OLS) are all approximately linear. These results suggest that, compared with EM and OLS methods, the multivariate copula modeled by RVM is closer to the empirical copula (the black line), no matter how the sample numbers change. Furthermore, all the steps above are aiming to calculate the wind power (P_w) accurately, which will be the input variables of PPF.

As the input variables consist of random variables, the computation result is the probabilistic power flow. The output information includes the probability distribution and digital characteristics of V, θ, P, and Q. Meanwhile, the calculation results acquired from the historical data of the wind farms are used as reference values. Thus, the relative errors of the expectation and standard deviation of the output variables are expressed as follows [38]:

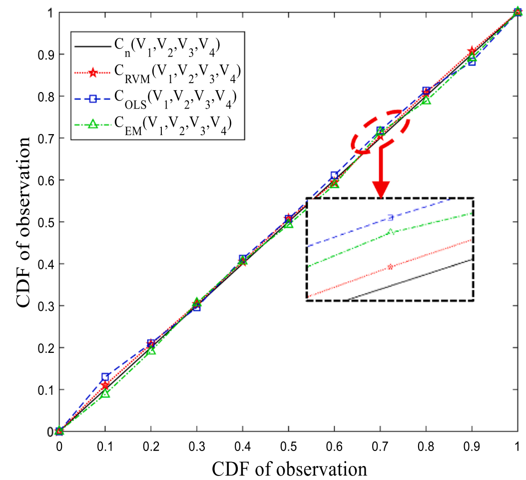

(a) Sample:2555

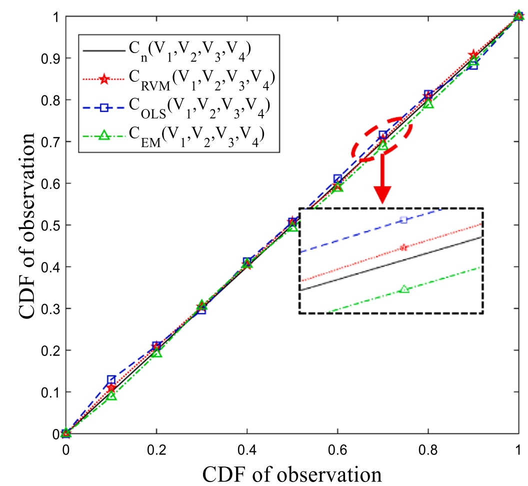

(b) Sample:8760

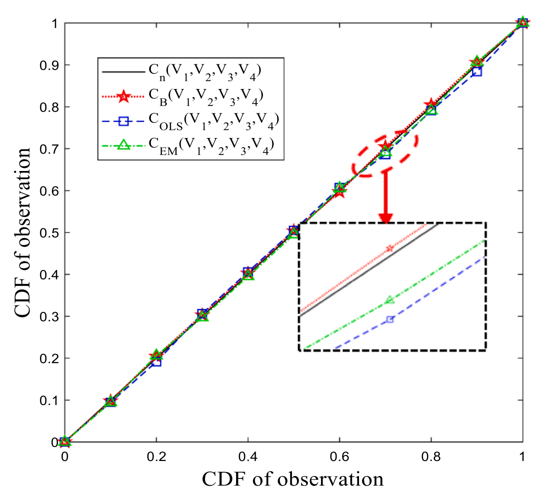

(b) Sample 52560

Fig. 2. P-P diagrams of the different methods.

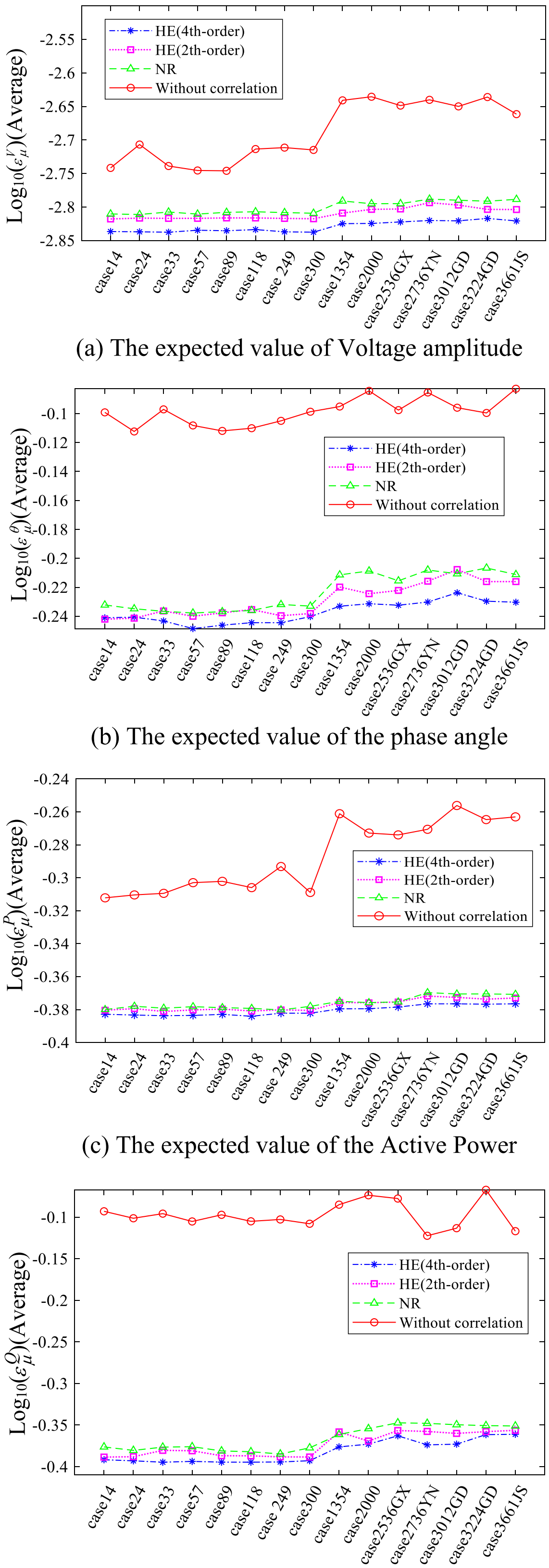

(a) The expected value of Voltage amplitude

(b) The expected value of the phase angle

(c) The expected value of the Active Power

(d) The expected value of the Reactive Power

Fig. 3. Error comparison of expected value.

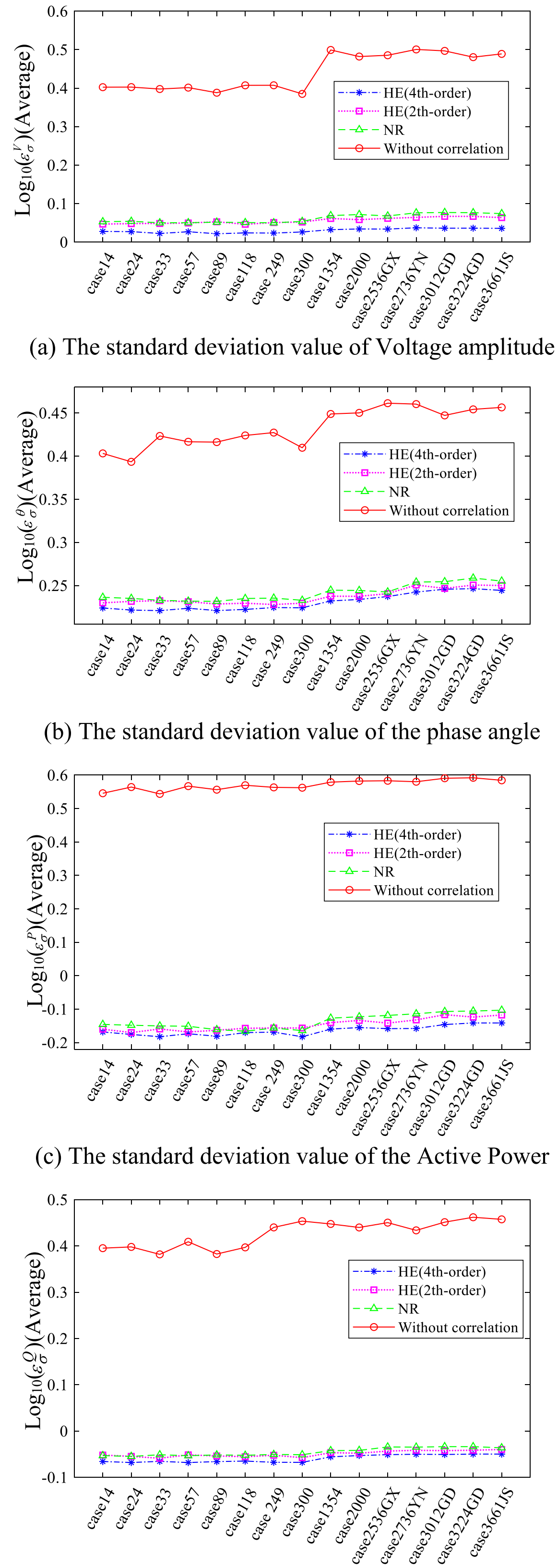

(a) The standard deviation value of Voltage amplitude

(b) The standard deviation value of the phase angle

(c) The standard deviation value of the Active Power

(d) The standard deviation value of the Active Power

Fig. 4. Error comparison of standard deviation.

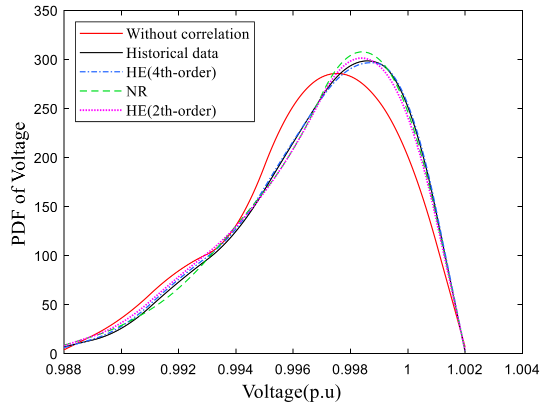

(a) In case33 system

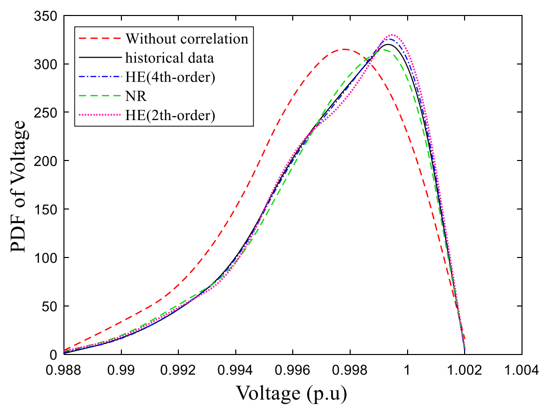

(b) In case3661 system

Fig. 5. The PDF of voltage.

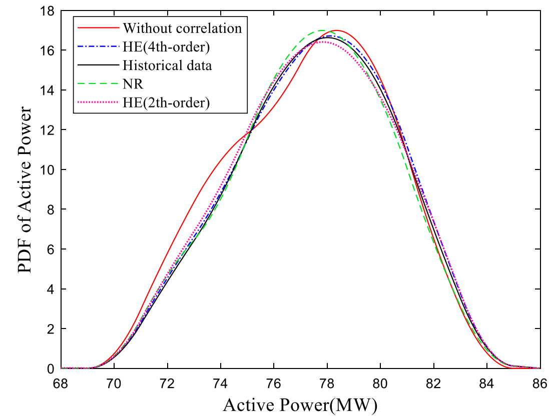

(a) In case33 system

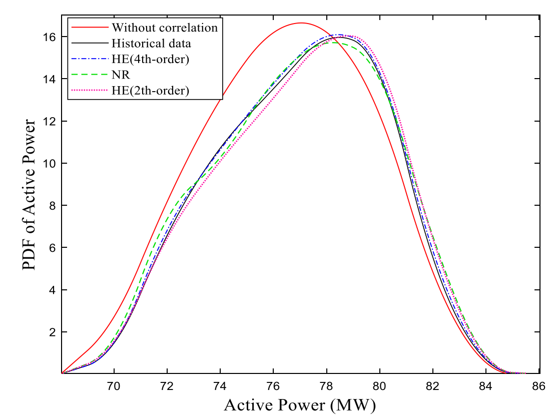

(b) In case3661 system

Fig. 6. The PDF of the active power.

$$\varepsilon_{\mu}^{x} = \left|\frac{\mu_{n}^{x} - \mu_{PEM}^{x}}{\mu_{n}^{x}}\right| \times 100\% \tag{40}$$

$$\varepsilon_{\sigma}^{x} = \left|\frac{\sigma_{n}^{x} - \sigma_{PEM}^{x}}{\sigma_{n}^{x}}\right| \times 100\% \tag{41}$$

where μ_{PEM}^{x}, μ_{n}^{x}, and σ_{n}^{x},σ_{PEM}^{x} represent the expected value and standard deviation obtained from the historical data and the proposed method, respectively. However, there are too many output variables of probabilistic power flow. This paper used the average and maximum of the relative error of each variable to measure the accuracy of the proposed method.

In order to demonstrate the impact of correlation among multivariate wind farms on the PPF of the power system, a comparative analysis was conducted. The cumulants ignored the correlation, and the cumulants based on the Newton–Raphson method considering the correlation were used to compare the proposed method. The results in Fig. 3 and Fig. 4 show that the average error of expectation and standard deviation calculated by cumulants based on the holomorphic embedding method is smaller than that obtained by the Newton–Raphson method. Such representation can be explained because the main practical features of the holomorphic embedding method are that it is non-iterative and deterministic, yielding the correct solution when it exists.

These figures also indicate that when ignoring the correlation between the wind farms, the PPF calculation results' error will be quite large. Therefore, it is more realistic to consider the correlation of multivariate wind farms for PPF analysis of the power system. Besides, it is clear that with the increase of the order of Padé approximant, the accuracy also improves. Nevertheless, it is important to note that a high order of Padé approximant will need more computing time. Therefore, the order should be limited to a specific range under the premise of ensuring accuracy.

Furthermore, the presented information shows that the proposed method limits the average relative error of the expected value to less than 2% and constrains the relative error of standard deviation to less than 3%, which demonstrates the accuracy of the proposed method. It is interesting to note that the error of standard deviation is greater than the error of the expected estimated value both in Fig. 3 and Fig. 4, which also conforms to the characteristics of the cumulants method. In addition, several PDF curves of bus voltage and active power in the branch are illustrated in Figs. 5 and 6. These diagrams also present the advantage of the proposed method because the curve of PDF depicted by the holomorphic embedding method is closer to the historical distribution than others.

In summary, there are two significant findings of the research. One is that the copula constructed by RVM can more actually reflect the correlation of wind farms than other traditional parameter estimation methods. The other is that the cumulants obtained from the holomorphic embedding method contribute to improving the accuracy of PPF calculation.

5. Conclusion

This paper predominantly focused on power flow calculation by considering multi-dimensional wind farms. A method based on RVM was proposed, which could accurately estimate the multivariate copula of wind speed between wind farms. Based on this, a new analytical cumulant developed by the HE method for accurate estimation of probability distributions for system variables. The results from simulation and published data support the following conclusions:

1) The correlation between wind speeds has a significant influence on the calculation results of PPF. However, compared with traditional estimation parameter methods, the RVM method can more accurately construct the multivariate copula for modeling the correlation of different wind farms and improve the computation speed to a certain extent.
2) The cumulant method based on holomorphic embedding gives an explicit nonlinear analytical power flow solution. Moreover, this method's main advantage is that it is non-iterative and is guaranteed to converge to the correct solution when it exists, which can retain more accurate probability distributions for system variables.
3) The results presented in Section IV confirm that in most cases, the proposed method showed a performance superior to the traditional NR method, even in large-scale models.

Declaration of Competing Interest

The authors declare that they have no known competing financial interests or personal relationships that could have appeared to influence the work reported in this paper.

Appendix A. Supplementary data

Supplementary data to this article can be found online at https://doi.org/10.1016/j.ijepes.2021.106843.

References

[1] Zhang Y, Wang J, Wang X. Review on probabilistic forecasting of wind power generation. Renew Sustain Energy Rev 2014;32:255–70.
[2] Liang Z, Liang J, Wang C, Dong X, Miao X. Short-term wind power combined forecasting based on error forecast correction. Energy Convers Manage 2016;119:215–26.
[3] Yu H, Chung CY, Wong KP, Zhang JH. Probabilistic load flow evaluation with hybrid Latin Hypercube sampling and Cholesky decomposition. IEEE Trans Power Syst 2009;24(2):661–7.
[4] Hajian M, Rosehart WD, Zareipour H. Probabilistic power flow by Monte Carlo simulation with Latin super cube sampling. IEEE Trans Power Syst May 2013;28(2):1550–9.
[5] Xie ZQ, Ji TY, Li MS, Wu QH. Quasi-Monte Carlo Based Probabilistic Optimal Power Flow Considering the Correlation of Wind Speeds Using Copula Function. IEEE Trans Power Syst March 2018;33(2):2239–47.
[6] Su CL. Probabilistic load-flow computation using point estimate method. IEEE Trans Power Syst Nov. 2005;20(4):1843–51.
[7] Morales JM, Perez-Ruiz J. Point estimate schemes to solve the probabilistic power flow. IEEE Trans Power Syst Nov. 2007;22(4):1594–601.
[8] Zhang P, Lee ST. Probabilistic load flow computation using the method of combined cumulants and Gram-Charlier expansion. IEEE Trans Power Syst Feb. 2004;19(1):676–82.
[9] Ruiz-Rodriguez FJ, Hernandez JC, Jurado F. Probabilistic load flow for photovoltaic distributed generation using the Cornish-Fisher expansion. Elect Power Syst Res 2012;89:129–38.
[10] Fan M, Vittal V, Heydt GT, Ayyanar R. Probabilistic power flow studies for transmission systems with photovoltaic generation using cumulants. IEEE Trans Power Syst Nov. 2012;27(4):2251–61.
[11] Stott B. Effective starting process for Newton-Raphson load flows. Proc Inst Electr Eng Nov. 1971;118:983–7.
[12] Chiang HD, Wang T, Sheng H. A Novel Fast and Flexible Holomorphic Embedding Power Flow Method. IEEE Trans Power Syst 2018;33(3):2551–62.
[13] Trias A. The holomorphic embedding load flow method. In: Proc Power and Energy Soc Gen Meeting, Jul. 2012, p. 1–8.
[14] Rao SD, Feng Y, Tylavsky DJ, Subramanian MK. The Holomorphic Embedding Method applied to the Power-Flow Problem. IEEE Trans Power Syst. 2016;31(5):3816–28.
[15] Trias A, J. L. Mar' ın. The holomorphic embedding load flow method for DC power systems and nonlinear DC circuits. IEEE Trans Circuits Syst I, Feb 2016;63(2):322–33.
[16] Liu C, Wang B, Xu X, Sun K, Bak CL. A Multi-Dimensional Holomorphic Embedding Method to solve AC Power. IEEE Access Nov 2017;5:25270–85.
[17] Freitas FD, Junior ACS, Fernandes LFJ, Acle YGI. Restarted Holomorphic Embedding Load Flow Model based o Low Order Padé Approximant and Estimated Bus Injection. Int J Electr Power Energy Syst, Comp Appl Nov 2019;112:326–38.
[18] Pessanha JFM, Melo ACG, Almeida VA. Impact of wind speed correlations on probabilistic power flow by using the Nataf transformation. In: Proc IEEE Int Conf 2018.
[19] Wang Z, Wang W, Liu C, et al. Probabilistic Forecast for Multiple Wind Farms Based on Regular Vine Copulas. IEEE Trans Power Syst 2017:1.
[20] Aas K, Czado C, Frigessi A, Bakken H. Pair-copula constructions of multiple dependence. Insurance Math Econ 2013;44:182–98.
[21] Bessa RJ, Miranda V, Botterud A, Zhou Z, Wang J. Imeadaptive quantile-copula for wind power probabilistic forecasting. Renew Energy 2012;40:29–39.
[22] Sun C, Bie Z, Xie M, Jiang J. Fuzzy copula model for wind speed correlation and its application in wind curtailment evaluation. Renew Energy 2016;93:68–76.
[23] Longa M. On mixtures of copulas and mixing coefficients. J Multivariate Anal 2015;139:259–65.
[24] Sklar A. Fonctions de repartition à n dimensions et leurs marges. Publication de l'Institut de Statistique l'Universite Paris 1959;8:229–31.
[25] Bedford T, Cooke RM. Vines—A New Graphical Model for Dependent Random Variables. Ann Statist. 2002;30(4).
[26] Jaworski AP, Durante F, Hardle W, Rychlik T. Copula theory and its applications. In: Proc. Workshop held in Warsaw, Poland, 25–26. New York, NY, USA: Springer; 2009. p. 25–6.
[27] Papaefthymiou G, Kurowicka D. Using copulas for modeling stochastic dependence in power system uncertainty analysis. IEEE Trans Power Syst Feb. 2009;24(1):40–9.
[28] Tipping ME. Sparse Bayesian learning and the relevance vector machine. J Mach Learn Res 2001;1:211–44.
[29] Xu F, Ma L, Wang J. A fault diagnosis method based on optimized RVM and information entropy for quadruped robot. In: Proc Chin Control Conf, Jul. 2016, p. 6617–22.
[30] Yang H, Xu Z, Ye J, King I, Lyu MR. Efficient sparse generalized multiple kernel learning. IEEE Trans Neural Netw Mar. 2011;22(3):433–46.
[31] Erven TV, Harremos P. Rényi divergence and Kullback-Leibler divergence. IEEE Trans Inf Theory 2014;60(7):3797–820.
[32] Conradsen K, Nielsen LB. Review of Weibull statistics for the estimation of wind speed distributions. J Appl Meteorol 1983;23(8):1173–83.
[33] Rosenblatt M. Remarks on a multivariate transformation. Ann Mathem Statist 1992;23(3):470–2.
[36] Jaschke S. The cornish-fisher-expansion in the context of delta-gamma-normal approximations. J Risk 2002;4(4):33–52.
[38] Verbic G, Canizares CA. Probabilistic Optimal Power Flow in Electricity Markets Based on a Two-Point Estimate Method. IEEE Trans Power Syst 2006;21(4).
[40] Xiao Yuanhui. A fast algorithm for two-dimensional Kolmogorov-Smirnov two-sample tests. Comput Stat Data Anal 2017.
[41] Gower JC. Properties of Euclidean and non-Euclidean distance matrices. Linear Algebra Appl 1985;67(none):81.